Carbon Balance
and Management

RESEARCH

Open Access

Simulation and control of regional construction land expansion incorporating carbon emissions

Zhiyuan Wang[1,2], Fan Wu[3*] and Zhengxuan Liu[4]

Abstract
As a major contributor to carbon emissions among various land-use types, the expansion and spatial distribution of construction land are critical factors in regional carbon management strategies. Although considerable research has independently examined construction land growth control and regional carbon emission assessments, few studies have integrated these aspects to guide construction land expansion within the framework of carbon peaking strategies. This study proposes an innovative framework that integrates carbon emission considerations into the management of regional construction land expansion. Using Changsha City as a case study, this research analyzes the spatiotemporal dynamics of construction land expansion and associated carbon emissions from 1990 to 2020, exploring their interdependencies. To project future trends, three scenarios—natural growth, high-emission expansion, and low-emission development—were developed to simulate the impacts of construction land changes on carbon emissions by 2030. The study evaluates the carbon emission consequences of urban expansion and proposes mitigation strategies within a low-carbon development framework. The findings indicate that: (1) From 1990 to 2020, construction land in Changsha City expanded by 660.24 km^2, primarily encroaching upon adjacent cultivated and forested lands. During the same period, carbon emissions increased by 1.3963×10^8 t, showing a strong positive correlation with construction land expansion; (2) By 2030, carbon emissions are projected to reach 2.396×10^8 t, 2.582×10^8 t, and 1.639×10^8 t under the natural growth, high-emission, and low-emission scenarios, respectively, reflecting increases of 53.21%, 65.11%, and 4.81% relative to 2020 levels; (3) Under both the natural growth and high-emission scenarios, construction land expansion is likely to intensify its adverse impact on the regional ecosystem, thereby reducing ecological stability. In contrast, the low-emission development scenario is projected to promote significant improvements in ecosystem health and resilience. This study offers critical insights for territorial spatial planning and construction land management within the context of the dual-carbon strategy, presenting a viable pathway for reconciling land expansion with ecological sustainability.

Keywords Construction land expansion, Carbon emission, Scenario simulation, Growth control, Changsha city

*Correspondence:
Fan Wu
wf19960913@163.com
[1]College of Landscape Architecture, Central South University of Forestry and Technology, Changsha 410004, China
[2]Hunan Big Data Engineering Technology Research Center of Natural Protected Areas Landscape Resources, Changsha 410004, China
[3]School of Architecture and Art, Central South University, Changsha 410004, China
[4]Delft University of Technology, Delft, Nederland

Introduction

Human-induced land-use change exerts a substantial influence on global climate and the carbon cycle [4, 6, 22]. Energy consumption and industrial activities generate substantial carbon dioxide (CO_2) emissions, which are closely associated with land-use patterns and their intensity. Unregulated expansion of construction land can disrupt regional ecosystem functioning, modify carbon-cycle processes, and pose significant challenges to sustainable development [1, 18, 28]. Since the Industrial Revolution, accelerated urbanization and industrialization have driven cumulative global carbon emissions to approximately 340 × 10^9 t by 2020; construction land–related activities account for over 90% (≈ 306 × 10^9 t) of this total [17], [5]. Therefore, effective management of urban construction land is essential for mitigating carbon emissions and advancing carbon-peaking and carbon-neutrality goals.

This study examines regional carbon emissions associated with land use using two analytical components: (1) carbon-emission accounting and forecasting and (2) spatiotemporal variation analysis and identification of influencing factors. Existing studies on land-use–related regional carbon emissions largely adopt these two perspectives. Regarding carbon-emission accounting and prediction, prior work has been conducted at multiple spatial scales, including regional [38] and provincial levels [27, 29], and across sectors such as energy [31, 39], transportation [26, 40], agriculture [8], and construction [10]. Scenario-based models have also been developed to project carbon-emission peaks. For example, Wu et al., [30] and Zhang and Zhao [37] analyzed the evolution of China's CO_2 emissions since the Reform and Opening-up period. They applied the Kaya identity and an extended STIRPAT model to examine relationships between carbon emissions and socioeconomic development and to project peak emissions. With the maturation of the field, carbon-emission accounting and forecasting should move beyond aggregate estimates to incorporate interregional linkages and scenario-specific emission patterns, thereby providing a more comprehensive and spatially explicit understanding of emission sources. For instance, Sun et al., [24] used a backpropagation (BP) neural network to predict CO_2 emissions in Hebei Province based on key drivers and validated the model's predictive performance. Similarly, Chen et al., [3] quantified carbon emissions in Beijing's transportation sector using 1990–2016 data and developed a support vector regression (SVR) model to forecast future emissions.

Research on spatiotemporal shifts in carbon emissions and their underlying drivers has increasingly examined how changes in regional land use shape emission patterns over time. The heterogeneity and mechanisms of carbon emissions are commonly examined by integrating land-use spatial patterns, temporal dynamics, and associated drivers. For instance, Xu et al. [32] and He et al. [9] used city-level data from China to estimate carbon emissions and applied spatial econometric models to examine spatial patterns and key drivers. Zhang et al. [35] developed an enhanced model that integrates a regression-based extension of Kaya's identity to quantify the direct and indirect effects of land-use expansion on regional carbon emissions and proposed planning strategies to mitigate these impacts. Liu et al. [13] and Cai and Li [2] analyzed spatiotemporal carbon-emission patterns, focusing on land-use transitions at the municipal and provincial levels, respectively. Building on these findings, they constructed factor-decomposition models to identify the determinants of spatial disparities in carbon emissions and concluded that construction land is a dominant contributor. Similarly, Li et al. [11] developed a factor-decomposition framework based on emission assessments to analyze temporal changes in construction land and energy consumption and to evaluate their association. However, relatively few studies have examined how carbon emissions respond to the expansion of construction land or how rising emissions may, in turn, constrain future land expansion. Focusing exclusively on the effects of land-use change on carbon emissions is insufficient to inform effective emission-reduction policies. Overall, existing studies have provided relatively systematic accounting and analysis of land-use–related carbon emissions across multiple spatial scales and disciplinary domains; however, important limitations remain. First, most studies emphasize carbon-emission accounting at macro-regional or sectoral scales while paying limited attention to the expansion of urban construction land—an essential process in territorial spatial planning—thereby hindering the characterization of the heterogeneous effects of construction-land growth and spatial evolution on carbon emissions. Second, prior research has largely interpreted emissions growth through land-use change and often assumes a unidirectional relationship; in contrast, studies that incorporate carbon-emission constraints into planning decisions—using them to guide the scale and spatial configuration of construction land—remain limited, which reduces the direct utility of the evidence base for low-carbon land-use regulation. Third, although many studies employ statistical analysis and model fitting, they are often weakly linked to territorial spatial planning practice; consequently, their findings are difficult to translate into operational zoning and regulatory strategies for construction land.

In 2020, the Chinese government announced the "dual-carbon" targets of peaking carbon emissions by 2030 and achieving carbon neutrality by 2060. A growing body of work advocates integrating these strategic objectives into land-use spatial planning frameworks [14, 32, 36]. At present, many Chinese cities are experiencing rapid urbanization, which often entails continued expansion of construction land to accommodate urban growth. Under the combined pressures of development demands and carbon constraints, achieving carbon peaking while sustaining economic growth remains a significant challenge. In November 2023, China's National Development and Reform Commission (NDRC) issued a notice launching the first batch of pilot cities for carbon peaking and designated Changsha, along with several other cities, as pilot sites. The pilot initiative is intended to create enabling conditions for greener urban development by testing carbon-peaking measures, thereby supporting the sustainable transition of regional economies and societies. As a major hub city in central China, Changsha has experienced sustained urbanization, accompanied by continued expansion of construction land. Consequently, the city faces pronounced spatial constraints and coordination pressures when reconciling urban land demand with carbon-mitigation targets. Meanwhile, forests, grasslands, and other ecological land uses occupy a substantial share of the municipal territory; therefore, construction-land expansion risks encroaching on carbon-sink areas. These characteristics make Changsha a representative case for examining the interplay between land-use change and the regional carbon balance. Accordingly, taking Changsha as the study area and adopting an integrated perspective that links territorial spatial planning with low-carbon development, this study examines the spatiotemporal evolution of carbon emissions induced by construction-land expansion during 1990–2020 and investigates the underlying mechanisms of spatial association. Building on this analysis, we develop a scenario-driven spatial simulation framework that integrates Monte Carlo methods with the Markov-PLUS model. We then specify three scenarios—business as usual, high-carbon development, and low-carbon development—to simulate construction-land expansion in 2030 and the associated carbon-emission responses. Furthermore, informed by the scenario results and from a planning-regulation perspective, we propose differentiated control strategies for construction-land growth, delineate priority and guidance zones for future expansion, and explore pathways for embedding emission-reduction targets into the spatial governance framework for construction land. The findings provide quantitative decision support for urban territorial spatial planning and for the rational management of construction-land growth under carbon-peaking objectives.

Study area and data sources

Study area

Changsha, located in eastern Hunan Province, China, lies between 111°53′–114°15′E and 27°51′–28°41′N. The municipality comprises nine administrative divisions—Furong, Tianxin, Yuhua, Kaifu, Yuelu, Wangcheng, Changsha County, Ningxiang, and Liuyang—with a total area of 11,849.94 km^2 (Fig. 1). Construction-land area increased from 257.80 km^2 in 1990 to 918.04 km^2 in 2020, representing a 356% increase. This rapid expansion has been accompanied by encroachment on forests, grasslands, and other land types with high carbon-sequestration capacity, potentially disrupting regional carbon balance and carbon-cycle processes. As the capital of Hunan Province and a core city in the middle reaches of the Yangtze River urban agglomeration, Changsha is undergoing rapid urbanization and has been designated as one of the first batch of national pilot cities for carbon peaking. Continued urban development is expected to further increase demand for construction land, placing additional pressure on ecological carbon sinks such as woodlands and grasslands. Assessing the impacts of construction-land expansion on urban carbon emissions is essential for supporting regional low-carbon development, guiding rational land expansion, and informing optimized urban spatial-planning strategies. In addition, the findings can provide a reference for other cities seeking to manage and mitigate urban carbon emissions under similar development pressures.

Data sources

This study primarily utilizes three categories of data: (1) Land use data. Landsat satellite imagery with cloud cover below 5% was employed to generate land use datasets for Changsha City across seven time points from 1990 to 2020. These data were obtained from the Resource and Environmental Science and Data Center of the Chinese Academy of Sciences (http://www.resdc.cn/Default.aspx). Land types were categorized into six classes based on national land use classification standards: agricultural land, woodland, grassland, construction land, water bodies (lakes and rivers), and unused land. The classification accuracy reached 91.3%, which meets the analytical requirements of this study. (2) Spatial driving factors. These datasets were derived from land use simulation outputs and were further refined using dynamic transportation analyses to incorporate spatial accessibility advantages. Socioeconomic data were obtained from the Resource and Environmental Science and Statistics Center, while demographic data were extracted from the Changsha Statistical Yearbook. (3) Carbon emission coefficients and land-use-specific energy consumption data. These datasets were acquired from the National Ecological Science Data Center (www.nesdc.org.cn) and the Changsha Energy Statistics Yearbook, and were resampled to a 30-meter spatial resolution. All aforementioned datasets were standardized using ArcGIS to ensure

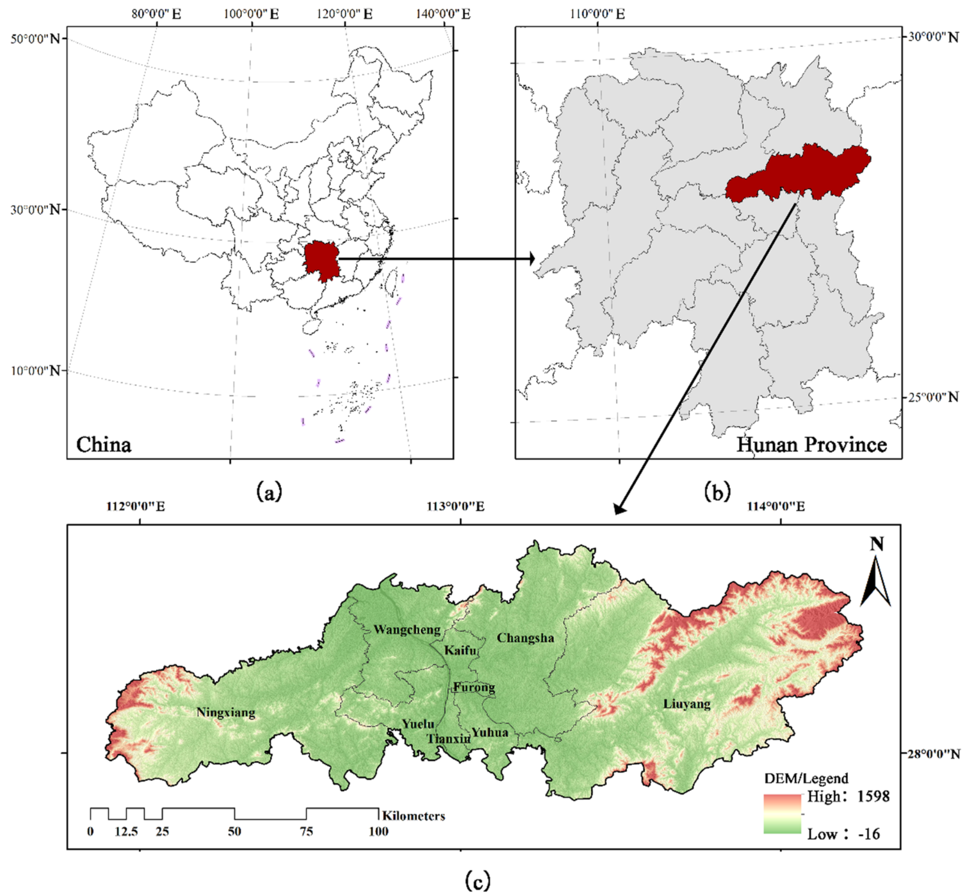

Fig. 1 Changsha City Location and City Limits

uniform raster dimensions in terms of row and column counts.

Research methods

This study proposes an integrated methodological framework that embeds carbon-emission constraints into the regulation of construction-land growth. The framework aims to elucidate coupling mechanisms between construction-land expansion and carbon-emission dynamics and to provide methodological support for low-carbon territorial spatial planning. Following the sequence "current-pattern identification–scenario-response simulation–translation into spatial regulation," the framework integrates construction-land change analysis, land-use–related carbon-emission accounting, and scenario-driven spatial simulation to establish an integrated analysis-and-forecasting system for planning support (Fig. 2).

(1) Current-pattern identification. Using land-use and activity data for Changsha during 1990–2020, we characterize construction-land expansion in terms of rate, intensity, and land-use transition pathways. Under a unified accounting scheme, we estimate land-use–related carbon emissions and examine their spatiotemporal patterns and association with construction-land expansion, thereby informing parameterization and constraint setting for subsequent scenario simulations.

(2) Scenario-response simulation. We construct a hierarchically coupled Monte Carlo–Markov–PLUS simulation framework, in which coupling is implemented primarily via scenario-based constraints on the projected quantity of construction land. The Monte Carlo module characterizes the probability distribution of total regional carbon emissions in 2030 under alternative development scenarios. Based on the statistical association between construction-land area and carbon emissions during 1990–2020, we translate carbon-emission scenarios into corresponding constraints on the total amount of construction land. Subject to these constraints, the Markov model projects the total construction-land area in 2030 and provides the projected total as an exogenous input to the PLUS model. Under the prescribed quantity constraint, the PLUS model allocates construction-land expansion spatially by incorporating land-use suitability, neighborhood effects, and explicit spatial constraints. Through this hierarchical coupling, carbon-emission scenarios impose ex ante constraints on construction-land area, thereby shaping spatial expansion patterns and enabling scenario-consistent characterization of

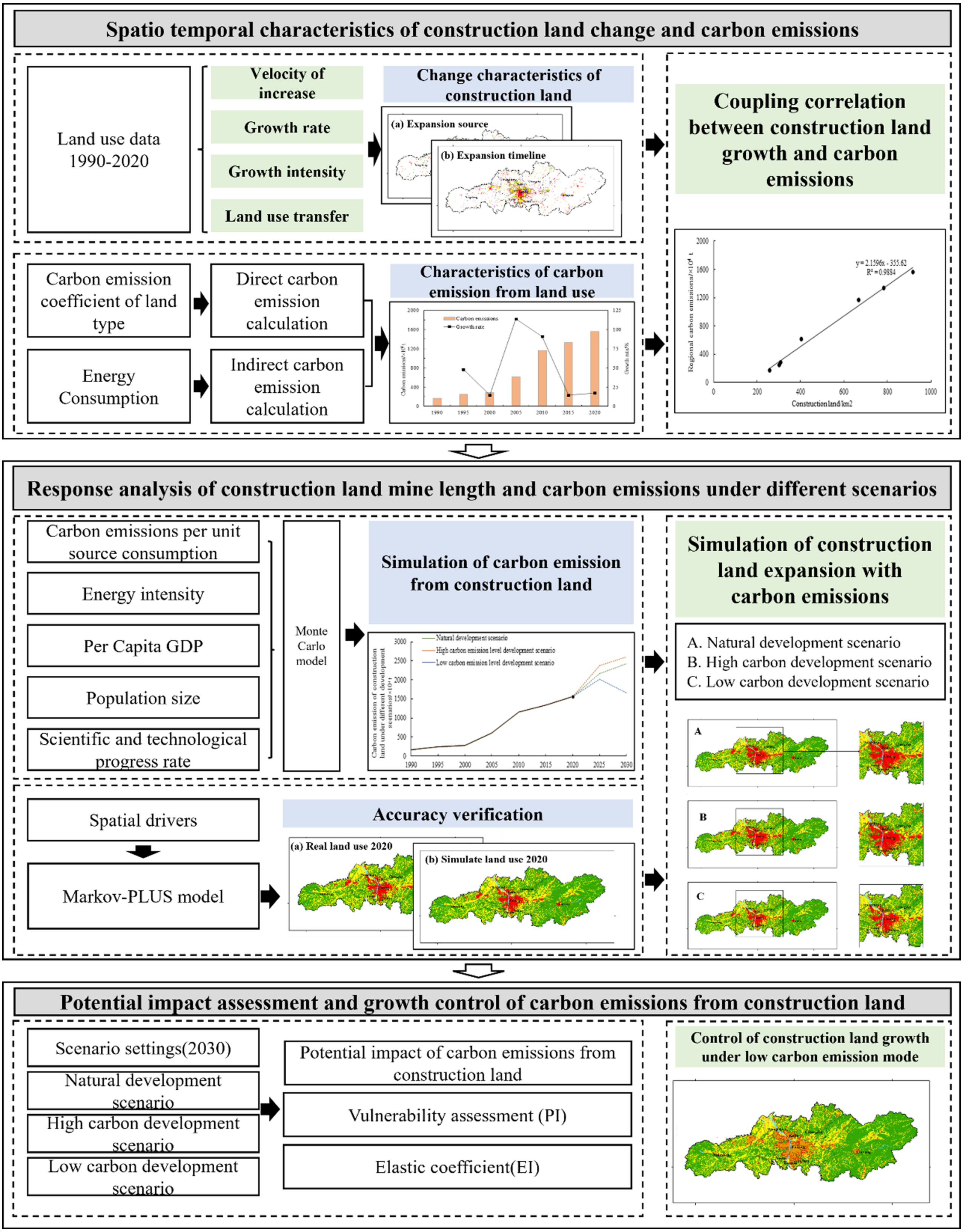

Fig. 2 Technical lines of research

construction-land expansion and carbon-emission responses.

(3) Translation into spatial regulation. Based on scenario-specific carbon-emission increments attributable to construction-land expansion and their spatial heterogeneity, we assess the implications of construction-land growth for regional carbon-balance objectives. From a territorial spatial planning and regulation perspective, we integrate expansion probability, carbon-emission intensity, and spatial constraints to delineate priority and guidance zones for construction-land growth and to propose differentiated regulatory strategies. The results provide quantitative evidence to support the formulation and implementation of urban territorial spatial plans aligned with carbon-peaking targets.

Measurement of changes in building land

To comprehensively characterize the expansion of construction land in the study area, we employed three indicators: growth rate, growth share, growth intensity and combined them with a land-use transition matrix to quantitatively assess changes in construction land. Specifically, the growth rate represents the mean year-to-year change in construction-land area; the growth share is defined as the expanded area relative to the initial (baseline) area, capturing relative changes in expansion magnitude; and growth intensity is the proportion of the expanded area to the total urban land area, indicating relative development pressure and the expansion pattern. Overall, the growth share emphasizes relative changes in expansion magnitude and thus enables a direct quantitative linkage to incremental carbon emissions; the growth rate helps identify critical phases of acceleration or deceleration, informing the prioritization of control measures; and growth intensity reflects relative development pressure, providing evidence for selecting the strength of planning controls and the necessity of spatial constraints. Together with the transition matrix, these metrics jointly support our objective of identifying construction-land growth characteristics under the "dual-carbon" constraint and proposing differentiated control strategies.

1. **Growth rate**

The growth rate of construction land measures the magnitude of change in construction land area per unit time, thereby indicating the overall scale and temporal trend of urban expansion. It also captures the direct quantitative effect of newly added construction land on land-use structure and carbon-emission changes. The formula is:

$$V = \frac{M_{n+i} - M_n}{n}$$

Where: The variable V denotes the rate at which construction land expands, M_{n+i} and M_n signify the construction land areas at years $n+i$ and n, respectively, with n indicating the duration of the interval in years.

(2) **Growth share**

The growth share of construction land enables comparisons of the relative magnitude and pace of construction land expansion across different periods, thereby identifying critical stages where expansion is closely associated with marked changes in carbon emissions. The structure of the equation essentially below:

$$I = \frac{M_{n+i} - M_n}{M_n} \times 100\%$$

Where: I denotes the growth share of construction land, M_{n+i} and M_n denote the construction land in years $n+i$ as well as i, correspondingly.

(3) **Growth intensity**

The city-scale development intensity metric serves as a measure of the increase in construction land within the same metropolitan region over different time periods, enabling a comparison of land growth characteristics within the same area over time [33]. This indicator also measures the development pressure imposed by construction-land expansion relative to the regional land base, enabling inter-period comparisons on a consistent and comparable basis. The formula is as follows:

$$U = \frac{A_{t_2} - A_{t_1}}{A_{t_1} \times \Delta t}$$

Where U denotes the construction land growth intensity index, A_{t1} and A_{t2} denote the area of construction land during time periods t_1 and t_2, respectively, and Δt represents the time interval between t_1 and t_2.

(4) Land use transfer.

Construction land transfer is used to represent the direction and extent of inter-conversion between different land use types during the study period. It includes the area of inflow and outflow between land categories upon completion of the research timeframe [20] while being calculated using the following formula:

$$S_{ij} = \begin{bmatrix} S_{11} & S_{12} & \cdots & S_{1n} \\ S_{21} & S_{22} & \cdots & S_{2n} \\ \vdots & & \ddots & \vdots \\ S_{n1} & S_{n2} & \cdots & S_{nn} \end{bmatrix}$$

Table 1 Carbon emission factors for each land-use type

Land use type	Carbon emission factor(t/hm^2)
Cropland	0.497
Woodland	−0.581
Grassland	−0.021
Water	−0.253
Unutilized land	−0.005

Where S denotes the extent of a specific land classification, n indicates the total count of classifications, while S_{ij} represents the matrix illustrating the transition of land area from category i at the study's outset to category j at its conclusion.

Measurement of carbon emissions from land utilization

Carbon emissions associated with land use are defined as an integrated representation of carbon emissions and carbon sequestration effects linked to land use patterns and their changes within the administrative boundary of the study area, as delineated in the corresponding annual statistical records. This definition covers both emissions arising from ecological and biogeochemical processes of different land cover types and emissions from energy consumption driven by human activities on construction land. In this study, emissions produced by ecological and biogeochemical processes of land cover types are referred to as direct emissions, while energy related emissions induced by human activities are referred to as indirect emissions. Direct emissions are estimated using an emission factor method by land use type, which characterizes the carbon source and sink effects of cropland, forestland, grassland, water bodies, and unused land; carbon sinks are allowed to take negative values to represent net ecosystem carbon uptake. Indirect emissions are calculated from the energy consumption statistics of the study area by converting energy use into standard coal equivalent and applying IPCC emission factors, thereby quantifying carbon emissions attributable to energy use on construction land.

(1) Direct carbon emission accounting

Considering the specific environmental and developmental context of Changsha City, carbon output associated with different land categories, including wooded areas, grasslands, croplands, watersheds, and unexploited terrain, is estimated using the direct emission coefficient method [21, 34, 39]. The formula for this estimation is presented below:

$$E_x = \sum{}_{i=1}^{n} A_i = \sum{}_{i=1}^{n} S_i \times T_i$$

Where: E_x refers to total direct carbon output (t); A_i denotes carbon emissions generated by category i (t); S_i represents the spatial extent of category i (km^2); and T_i signifies the emission coefficient for category i (as detailed in Table 1) in t/km².

(2) Indirect Carbon Emission Accounting

The carbon footprint of construction processes is assessed by initially converting energy consumption from industrial production and daily human activities into tons of standard coal equivalents. Carbon output is then derived based on the emission coefficients associated with various energy sources, as specified in the IPCC guidelines and corroborated by existing research [19]. Using energy consumption data for Changsha(The dataset covers the period 1990–2020 and was compiled from the *Changsha Energy Statistical Yearbooks* and publications of the Changsha Municipal Bureau of Statistics), this study estimates emissions from nine primary energy sources utilized in industrial operations and daily life, including coal, petroleum, and natural gas. The emission calculation is determined by the following equation:

$$E_y = \sum{}_{i=1}^{n} B_i = \sum{}_{i=1}^{n} Pn_i \times M_i \times Q_i$$

Where: E_y denotes total indirect carbon output, specifically emissions linked to developed land (t); B_i represents the emissions associated with energy category i (t); Pn_i indicates the consumption volume of energy category i, measured in tons(t); M_i is the conversion coefficient from the i-th energy type to standard coal; and Q_i is the carbon emission coefficient of the i-th energy type. The details are provided below (Table 2).

Table 2 Energy carbon conversion factor

Carbon source	Conversion factor for standard coal	Carbon emission factor
Raw Coal	0.7140 kg·kg^{-1}	0.7559
Coke	0.9714 kg·kg^{-1}	0.8550
Natural Gas	1.4714 kg·kg^{-1}	0.4483
Gasoline	1.4714 kg·kg^{-1}	0.5538
Kerosene	1.4714 kg·kg^{-1}	0.5714
Diesel oil	1.4714 kg·kg^{-1}	0.5921
Fuel Oil	1.4714 kg·kg^{-1}	0.6185
Heat	0.0341 kg·(10^{6}J^{-1})	0.7330
Electricity	0.1229 kg·(kW·h)$^{-1}$	0.7330

Monte Carlo simulation based on carbon emission decomposition factor modeling

(1) Monte Carlo model setup

Monte Carlo simulation can randomly sample values from multiple variables based on specified probability distributions, combining them for operations. This method offers advantages in multi-scenario analysis and uncertainty assessment [25]. By combining numerous randomly generated scenarios, the Monte Carlo simulation can model the diverse evolution paths of urban carbon emissions, thereby identifying the most likely carbon peak conditions and emission reduction potentials for a city. This provides more reliable data and research support for urban carbon peak action plans. The Monte Carlo simulation allows for the visual identification of the most probable carbon peak and reduction potentials in a city, offering more reliable data and research support for the city's carbon peak action plan. The traditional Kaya equation considers only the impacts of energy, economy, and population on carbon emissions, neglecting the influence of scientific and technological progress. Therefore, this study uses 0.91 times the rate of change in labor compensation to represent the rate of scientific and technological progress, constructing a Monte Carlo model based on this approach. The specific mathematical formulation is as follows:

$$C_z = C_e \times k = \frac{C_e}{MC_e} \times \frac{MC_e}{GDP} \times \frac{GDP}{P} \times P \times k$$

Where C_z represents total carbon emissions, C_e denotes carbon emissions derived from energy use, MC_e indicates overall energy utilization, while *GDP* signifies economic output, P corresponds to the total population, and k eflects advancements in science and technology. Based on the above, define $\alpha = \frac{C_e}{MC_e}$, $\beta = \frac{MC_e}{GDP}$, and $\gamma = \frac{GDP}{P}$. The equation can then be

$$C_z = \alpha \times \beta \times \gamma \times P \times k$$

.

where α, β, γ, P, and k represent carbon emissions per unit of energy use, energy consumption efficiency, economic output per person, total population size, and the pace of scientific and technological advancements, respectively.

(2) Carbon emission scenario setting for construction land use

Monte Carlo simulation, through repeated sampling of random sequences, is used to explore the probability distribution of different variables within a given interval and to identify evolutionary paths based on logical deduction. This study adopts 2020 as the base period and sets up three scenarios: natural development, high-carbon natural progression, high-carbon growth, and low-carbon transformation. The rate of change for the base period (2020) is established as follows: According to the Changsha Municipal Statistical Yearbook and the Changsha Municipal National Economic and Social Development Statistical Bulletin, Changsha's total energy consumption in 2020 was 272,886,440 tons, with a GDP of 1,214,252 million Yuan and a population of 1.0479 million. The rates of change for carbon emissions from energy consumption, energy intensity, GDP per capita, and technological progress are – 29.57%, −17.5%, −17.5%, and 13.35%, respectively. The other two scenarios—the scenario with high carbon emissions and the one with low carbon emissions—are simulated using these parameters.

Scenario 1: Natural Development Scenario

The natural growth scenario is established using the spatiotemporal patterns of carbon emissions associated with Changsha's construction land from 1990 to 2020. This scenario assumes unchanged influencing factors and growth rates, with no modifications aligned with prevailing trends. The highest, lowest, and median values recorded during 2005–2019, 2010–2019, and 2015–2019 serve as key quantitative indicators for these influencing factors (Table 3).

Table 3 Rate of change of carbon emission factors under different development scenarios(%)

Scenarios	Target	2020–2030					
		2020–2025			2025–2030		
		Maximum value	Intermed-iate value	Maximu-m value	Maxim-um value	Inteme-diate value	Maxi-mum value
Natural Development Scenario	α	−4.70	7.34	12.49	−4.70	7.34	12.49
	β	−19.62	−13.98	3.37	−19.62	−13.98	3.37
	γ	1.10	16.87	25.99	1.10	16.87	265.99
	k	−2.36	−1.81	−1.27	−2.36	−1.81	−1.27
High Carbon Emission Level Development Scenario	α	8.94	9.34	9.74	9.54	9.84	10.14
	β	−12.38	−11.98	−11.58	−11.78	−11.48	−11.18
	γ	18.47	18.87	19.27	19.07	19.37	19.67
	k	−0.20	0.20	0.60	0.40	0.70	1.00
Low Carbon Emission Level Development Scenario	α	5.54	6.34	7.14	4.74	5.34	5.94
	β	−15.78	−14.98	−14.18	−16.58	−15.98	−15.38
	γ	15.07	15.87	16.67	14.27	14.87	15.47
	k	−3.6	−2.81	−2.01	−4.41	−3.81	−3.21

Scenario 2: High-Carbon Development Scenario

This scenario is formulated based on the Changsha New Urbanization Development Plan (2021–2025), the Three-Year Action Plan for Integrated Development of Changzhutan (2023–2025), and the Changsha Territorial Spatial Master Plan (2021–2035). It projects that by 2025, Changsha's GDP will reach 184.5 billion yuan, with an estimated resident count of 11.7 million. By 2035, the city's population is expected to expand to 15.5 million, accompanied by accelerated modernization and industrial growth, driving an increase in economic expansion rates. Detailed parameter configurations are provided in Table 3.

Scenario 3: Low-Carbon Development Scenario

As outlined in the Changsha City Carbon Peak Implementation Plan, the share of non-fossil energy consumption is set to surpass 20% by 2025 and 22% by 2030, which remains 3% points below the provincial target. The energy efficiency of large-scale industrial enterprises in the city is projected to improve, with energy use per unit of added value declining by 14.5% by 2025, as specified in the Changsha "14th Five-Year" Energy Efficiency and Emission Reduction Action Plan. Additionally, under the Changsha Peak Carbon Implementation Program and national guidelines for pilot cities striving to reach peak emissions, the city aims for a 15% reduction in energy use intensity per unit of GDP by 2025, using 2020 levels as a benchmark. By 2030, energy intensity relative to GDP will continue to decline, while the rate of CO_2 emission reduction per unit of economic output will align with provincial targets. Furthermore, forest coverage, encompassing tree and green space density, is planned to remain stable at 55%. Based on these policy objectives, specific indicator values for key influencing factors are determined (Table 3).

Construction land simulation (Markov-PLUS model)

(1) PLUS model setup

The PLUS model is a state-of-the-art tool for simulating land use changes. Its workflow involves data conversion, identification of spatial variations, and predicting land suitability through random forest algorithms. Additionally, the model employs an adaptive inertia mechanism to determine spatial allocation and subsequently validates the simulation results. A detailed description of the operational mechanisms and the parameters can be found in Table 4. Previous research has shown that the PLUS model is more effective in predicting future spatial changes in land use [12].

(2) Scenario setting

Table 4 PLUS model parameterization

Module type	Module Parameters	Operation Settings	Parameter description
The information conversion, land expansion extraction for regional construction	Land extension clearance	-	Integrating the 1990 and 2020 study area data into the database
An research approach for land use growth utilizing Random Forest	Land expansion map	Information collected on residential land expansion for the 1990–2020 study territory	-
	Directory encompassing driving forces	Driver Folders	-
	Quantity of regression tree branches	Count of decision trees	20
	The act of sampling rate	Sampling ratio	0.01
	mTry	Number of features utilized for training the decision tree	16
Allocating space via the adaptive inertia mechanism	Possibilities towards growth	Variability in frequency of the site's suitability for each type of site	Land use appropriateness probability produced by the random forest algorithm
	Structure of property utilization	The study area's status quo data (which requires format conversion)	Input 2020 land use data
	Restrictions of conversion	limited development space (format conversion required)	Information on the research area's present rivers, lakes, basic cropland, and ecological protection zones
	Output Path	Save Path	
	Extent of the community	Neighborhood range	3*3
	Patch generation	Ease of site conversion and decay coefficient of lowering threshold (0 ~ 1)	0.9
	Expansion coefficient	The greater the random patch probability (0 ~ 1), the more probable it is that additional patches will be created.	0.1
Accuracy validation	Kappa Coefficient Overall Acuracy		Comparison of the real land use distribution with the simulation results

Utilizing the Monte Carlo and Markov-PLUS models and considering the region's economic trajectory, three alternative pathways for construction land transformation from 2020 to 2030 are introduced: natural growth, intensive carbon expansion, and low-emission development. The natural growth model assumes a continuation of land use dynamics and carbon emission trends observed from 1990 to 2020, where population increase, energy demand, economic output, and land development progress in alignment with existing patterns. The high-carbon development scenario seeks to increase urbanization and economic development through rapid land expansion, without considering the impact of carbon emissions on regional development. The low-carbon development scenario focuses on achieving or surpassing the carbon emission reduction targets set by Hunan Province, with ecological protection as the primary consideration.

Potential impact analysis

(1) Potential impact assessment (PI)

Ecological vulnerability refers to a system's susceptibility and limited capacity to adapt to the adverse impacts of climate change. Schroter et al., later expanded this concept to include the effects of land transformation [15]. Drawing from the IPCC report and Schroter et al.'s definition of ecological vulnerability [23], this study applies the methodology proposed by Metzger et al., [16] to evaluate the susceptibility of land use alterations to ecosystem functionality. To quantify the risk to carbon stock services within ecosystem hubs, the Potential Impact Index (PI) is employed, calculated as follows:

$$\mathrm{PI} = \frac{\Delta C}{\Delta L}$$

Where ΔL denotes the variation in the land-use index, and ΔC signifies the alteration in carbon stocks(t).The land-use index serves as a metric to assess the interplay between anthropogenic activities and the natural environment. An elevated index value suggests intensified human influence on the environment and a more advanced stage of urbanization. The calculation of this index follows the formula below:

$$L = 100 \times \sum{}_{i=1}^{n} D_i \times P_i$$

In this formula, D_i denotes the grading index corresponding to the land-use degree at level i, with values assigned based on relevant studies: unutilized land is assigned a value of 1, ecological land (e.g., forests, grasslands, and watersheds) is given a value of 2, arable land is designated as 3, and construction land is classified as 4. Meanwhile, P_i represents the proportion of the total area occupied by each land-use category.

(2) Coefficient of elasticity (EI).

Elasticity refers to the proportional change in one variable relative to another. It is commonly employed to assess how the growth rate of one economic variable correlates with the growth rate of another within a defined time frame. Building on this concept, a model was formulated to evaluate the relationship between construction land expansion and carbon emissions within the study area, quantifying carbon emission responses under various analyzed scenarios. The corresponding calculation formula is as follows:

$$\mathrm{EI} = \frac{\Delta C_{i+n}}{C_i} / \frac{\Delta S_{i+n}}{S_i}$$

In this formula, *EI* represents the carbon emission response intensity of construction land, also known as the elasticity coefficient. ΔC_{i+n} represents the variation in carbon emissions from construction land between the *(i + n)-th* year and the *i-th* year, while C_i indicates the carbon emissions from construction land in the *i-th* year. Similarly, ΔS_{i+n} signifies the change in construction land area over the same period, whereas S_i corresponds to the construction land area in the *i-th* year.

Analysis of results

Spatiotemporal analysis of construction land dynamics and associated carbon Emissions

Characterization of changes in construction land

This study analyzes the expansion of construction land in Changsha City from 1990 to 2020, using growth rate and growth intensity as key statistical indicators (Table 5). During the study period, the area of construction land increased from 257.80 km² to 918.04 km², with its share of the total land area rising from 2.17% to 7.77%, corresponding to a cumulative growth rate of 356%. The overall growth rate and intensity exhibited a fluctuating pattern, initially increasing and later declining, indicating distinct phases of expansion. Notably, between 2005 and 2010, construction land expanded by 667.31 km², with the peak annual increase reaching 263.74 km²—accounting for 34.00% of the total increase over the entire study period. Forest land and cultivated land were the primary sources of construction land conversion, jointly contributing 818.65 km², or 95.82% of the total expansion. Specifically, the converted area rose from 26.39 km² in 1990–1995 to a peak of 309.20 km² during 2005–2010, before declining to 182.25 km² in 2015–2020. This pattern is consistent with the general trajectory of construction land expansion.

In terms of spatial distribution (Fig. 3), construction land is mainly concentrated in areas of gentle topography,

Table 5 Construction Land Growth and Land Class Shift in Changsha, 1990–2020

Year	Area of growth	Growth speed	Growth rate	Intensity of growth	Category-specific transfers		
					Category Name	Transfer out	Transfer in
1990–1995	44.98	8.996	17.45	0.08	Cropland	2.62	21.74
					Woodland	1.23	4.65
					Grassland	0.01	0.00
					Water	0.09	4.35
					Unutilized land	0.00	0.00
1995–2000	5.83	1.166	1.93	0.01	Cropland	20.41	15.92
					Woodland	5.923	17.64
					Grassland	0.02	0.045
					Water	2.81	1.26
					Unutilized land	0.00	0.00
2000–2005	94.96	18.992	30.78	0.16	Cropland	8.48	51.13
					Woodland	4.06	52.69
					Grassland	0.04	0.49
					Water	0.64	3.97
					Unutilized land	0.00	0.00
2005–2010	263.74	52.748	65.35	0.45	Cropland	33.28	175.44
					Woodland	20.42	133.76
					Grassland	0.17	1.40
					Water area	4.72	11.82
					Unutilized land	0.16	0.09
2010–2015	115.32	23.064	17.28	0.20	Cropland	30.85	94.65
					Woodland	21.31	68.78
					Grassland	0.34	0.56
					Water area	2.97	6.73
					Unutilized land	0.033	0.04
2015–2020	135.41	27.082	17.30	0.23	Cropland	24.81	99.50
					Woodland	23.58	82.75
					Grassland	0.36	0.67
					Water area	2.91	4.03
					Unutilized land	0.02	0.23

displaying a typical outward growth pattern from the city center to the periphery. Recent construction activities have been concentrated in the central Furong District, eastern Changsha County, and the urban cores of Liuyang and Ningxiang Cities. This expansion trend is primarily driven by rapid urbanization and industrialization, which have intensified economic and social activities in central areas, thereby stimulating development in surrounding regions and accelerating the expansion of construction land.

Characteristics of carbon emissions from land use

Based on land use and energy consumption data from 1990 to 2020, both direct and indirect carbon emissions in Changsha City were quantified (Table 6). Over the study period, total carbon emissions increased substantially, while the carbon sink capacity associated with land use remained limited. Net carbon emissions rose from 1.6810×10^6 t to 1.5641×10^7 t by 2020, representing a 9.3-fold increase. As illustrated in Fig. 4, the growth trend of net carbon emissions closely mirrored the fluctuating pattern of construction land expansion. Among the two primary land-use-related sources of emissions in Changsha, construction land overwhelmingly dominated, with its share increasing from 91.16% in 1990 to 98.95% in 2020. This indicates that ongoing urbanization and industrialization are likely to further accelerate the expansion of construction land, thereby contributing to rising carbon emissions. In contrast, reductions in cultivated land area were associated with a slight decline in carbon emissions. Specifically, emissions from cultivated land decreased by 1.93×10^4 t over the study period. Therefore, construction land remains the principal source of carbon emissions in Changsha and is expected to continue as the dominant contributor amid ongoing urban expansion.

Coupled correlation analysis of construction land expansion and carbon emissions

Construction land, which supports the majority of human activities—major contributors to carbon emissions—exhibits a strong and consistent correlation with regional carbon emissions. This relationship is confirmed through

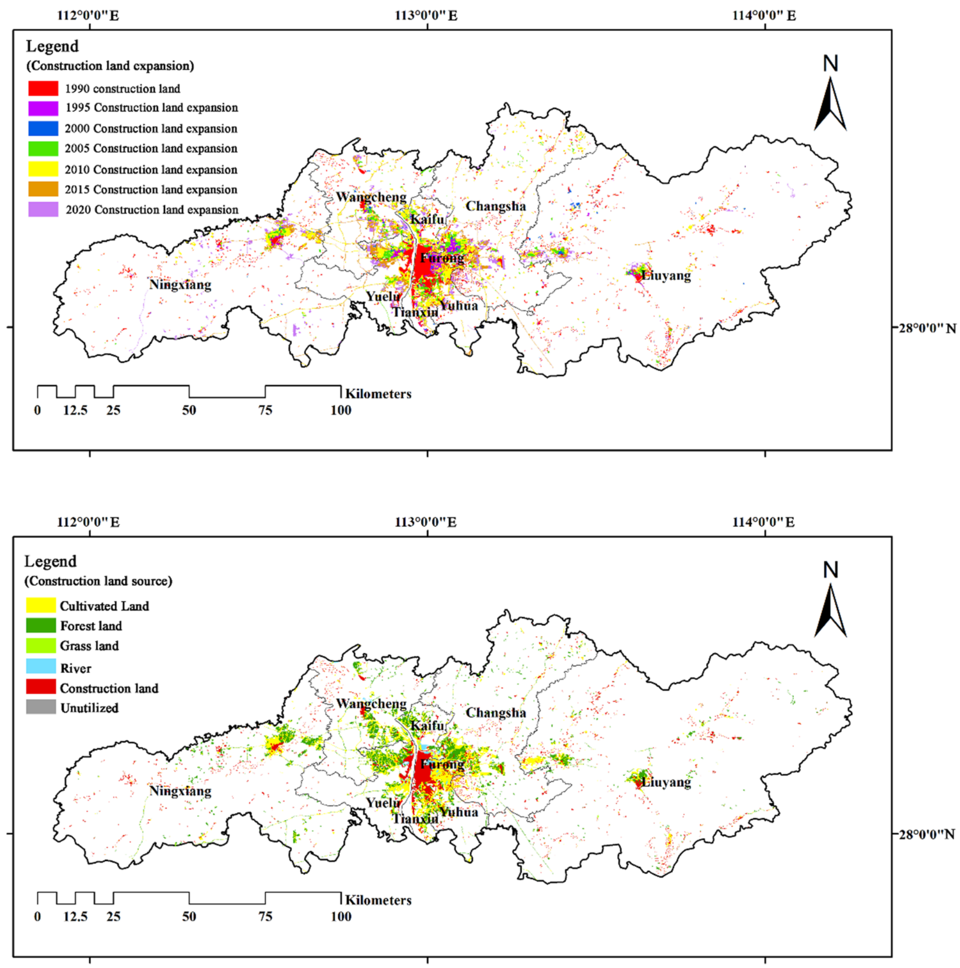

Fig. 3 Changes in Construction Land Expansion in Changsha, 1990–2020

Table 6 Changes in Carbon Emissions in Changsha, 1990–2020

	Cropland (×10^{4}t)	Woodland (×10^{4}t)	Grassland (×10^{4}t)	Water (×10^{4}t)	Construction Land(×10^{4}t)	Net carbon emissions (×10^{4}t)
1990	18.72	−42.94	−0.03	−0.63	192.98	168.10
1995	18.57	−42.94	−0.03	−0.60	273.94	248.94
2000	18.58	−42.86	−0.03	−0.63	310.17	285.23
2005	18.30	−42.55	−0.03	−0.64	634.57	609.66
2010	17.52	−41.90	−0.03	−0.64	1189.75	1164.70
2015	17.18	−41.66	−0.03	−0.64	1357.83	1332.69
2020	16.79	−41.30	−0.03	−0.65	1589.28	1564.09

statistical analysis of the spatiotemporal dynamics of construction land expansion and carbon emission trends in Changsha. Regression analysis (Fig. 5) reveals a strong positive correlation, with an R^2 value of 0.9884. The corresponding regression equation is: $y = 2.1596x - 355.62$, where x denotes the construction land area (km^2) and y represents regional carbon emissions (×10^4 t). The correlation indicates that construction land expansion and carbon emissions evolve synchronously over time, but it does not necessarily imply a one way causal relationship. During the study period, the share of emissions attributable to construction land increased steadily. This is partly because construction land concentrates energy intensive processes such as population agglomeration, industrial production, and transport, leading to substantially higher emissions per unit area than ecological land; therefore, expansion can raise total emissions directly through increased energy consumption. In addition, expansion often occurs at the expense of high sequestration land such as forests and grasslands, which weakens regional carbon uptake capacity. As a result, carbon emissions may increase more rapidly due to the

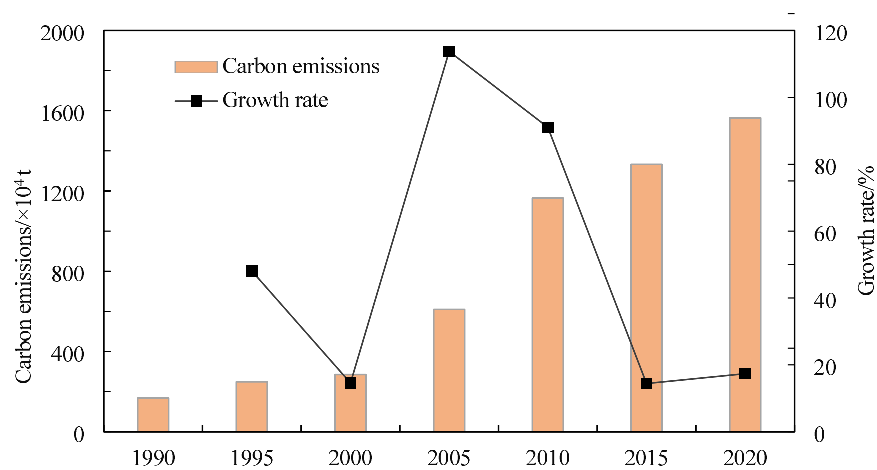

Fig. 4 Changsha Net Carbon Emissions and and Net Carbon Emissions Growth Rate

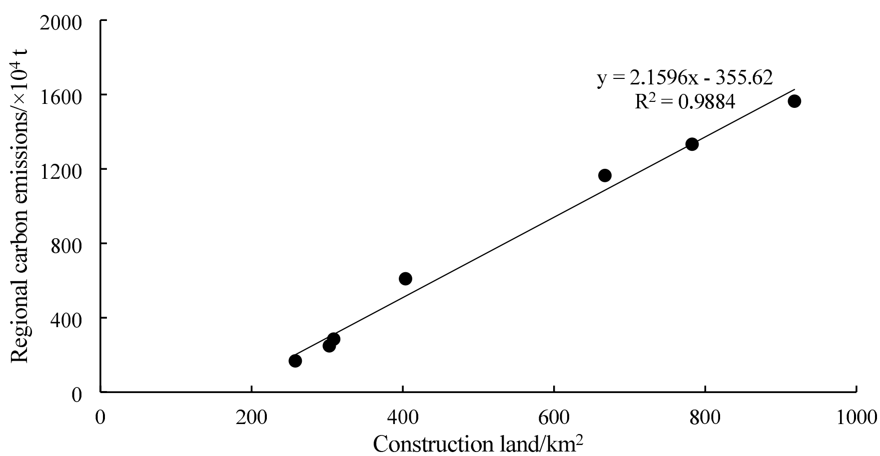

Fig. 5 Analysis of the correlation between building land and regional carbon emission fitting

combined effect of higher emissions and reduced carbon sinks. Accordingly, the subsequent scenario simulations consider not only changes in the scale of construction land but also differences in carbon balance effects arising from its encroachment on ecological space.

Analysis of building land expansion and carbon emission response under different scenario simulations

Construction land carbon emission simulation

A Monte Carlo simulation was employed to model carbon emissions from construction land in 2030, aiming to assess the emission response to Changsha's construction land expansion. Based on predefined scenario variables, iterative simulations were conducted to generate carbon emission projections under three urban expansion scenarios (Fig. 6).

By 2030, regional carbon emissions in Changsha are projected to increase under all three development scenarios compared to 2020, with the most pronounced growth occurring in the high-emission scenario. Under the natural development scenario, and without external policy intervention, carbon emissions from construction land are expected to increase steadily, reaching 2.42108×10^7 t by 2030—an increase of 8.5699×10^6 t or 54.19% over 2020 levels.

In the high-emission development scenario—characterized by a focus on economic growth, reduced emphasis on low-carbon initiatives, intensified industrialization, and accelerated urbanization—carbon emissions are projected to rise by 1.04318×10^7 t, corresponding to a 66.70% increase over 2020 and an average annual increment of 1.0432×10^6 t.

In contrast, the low-emission development pathway—which prioritizes land use control, industrial restructuring, and improvements in energy efficiency—exhibits a fluctuating emission trajectory. Emissions under this

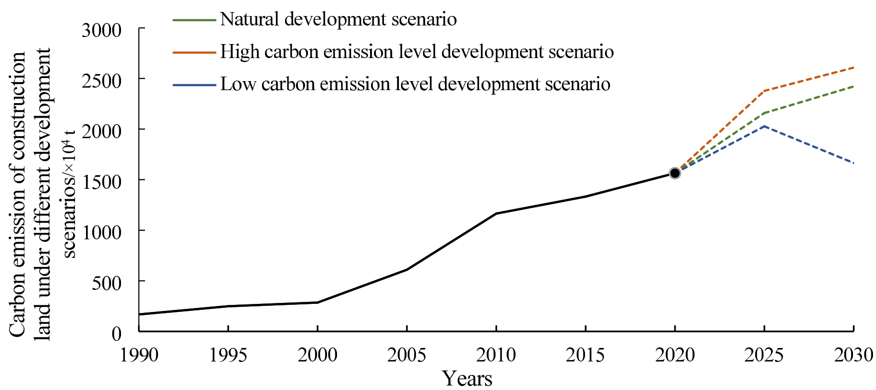

Fig. 6 Projections of carbon emissions from construction land in Changsha in 2030 under different scenarios

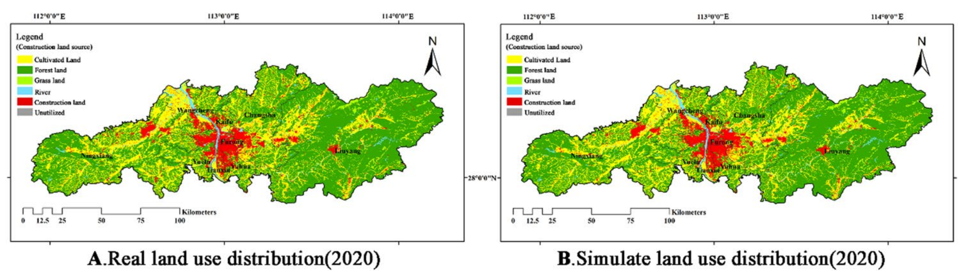

Fig. 7 Validation of the accuracy of the simulation of the distribution of building land expansion (2020)

scenario are projected to peak at 2.02688×10^7 t in 2025 before declining to 1.66449×10^7 t by 2030, resulting in a net increase of only 1.0041×10^6 t over 2020, equivalent to a growth rate of 6.42%.

The divergence in carbon emission trajectories across the three scenarios fundamentally reflects the combined effects of economic growth, energy efficiency, and technological progress on the emissions side, as well as the indirect influence of construction land expansion patterns on the carbon sink side. Under the natural development and high carbon development scenarios, the expansion of economic activity and the advance of urbanization drive simultaneous growth in energy consumption and demand for construction land. Meanwhile, the conversion of ecological land reduces regional carbon sequestration capacity, resulting in a sustained rise in emissions. In the low carbon development scenario, constraints such as a decline in energy intensity per unit of GDP, industrial structure upgrading, and a higher share of non fossil energy suppress the growth rate of emissions. At the same time, the scale and spatial configuration of construction land expansion are constrained, which reduces encroachment on high sequestration land and leads emissions to peak in the medium term before declining.

Simulating construction land expansion under multiple scenarios with carbon emission considerations

(1) Verification of construction land expansion simulation accuracy

This study simulates the spatial distribution of construction land in 2020 using the 2015 land use layout of Changsha as the baseline. The projected outcomes are illustrated in Fig. 7. To evaluate the model's accuracy, the construction land simulation generated by the PLUS model for 2020 was compared with observed land use data from the same year. The validation results show an overall accuracy (OA) of 0.95 and a Kappa coefficient of 0.91, indicating high model reliability and suitability for future construction land projections.

(2) Simulation of construction land expansion under multiple scenarios

The total land area of Changsha serves as the baseline reference for land use optimization. The Monte Carlo and Markov models are applied to simulate land demand under different carbon emission scenarios. Additionally, the PLUS model is used to project land use patterns and simulate construction land expansion within the study area under three development scenarios: Natural Development, High-Emission Growth, and Low-Emission Growth (Table 7; Fig. 8). Under the Natural Development scenario, construction land expands to 1,285.89 km², accounting for 10.89% of the total area—an increase of 40.07% relative to 2020. In the High-Emission scenario,

Table 7 Land use changes in the study area in 2030 under different scenarios

Land use type	Changsha land use status in 2020 (km^2)	Natural development scenario in 2030 (km^2)	High Carbon Emission Development Scenario 2030 (km^2)	Low Carbon Emission Development Scenario 2030 (km^2)
Cropland	3377.52	3221.28	3182.96	3377.73
Woodland	7109.02	6935.26	6900.97	7094.66
Grassland	137.96	137.55	137.41	137.93
Water	255.41	221.02	207.04	255.36
Construction Land	918.12	1285.89	1372.11	935.51
Unutilized land	6.45	7.72	8.24	7.54

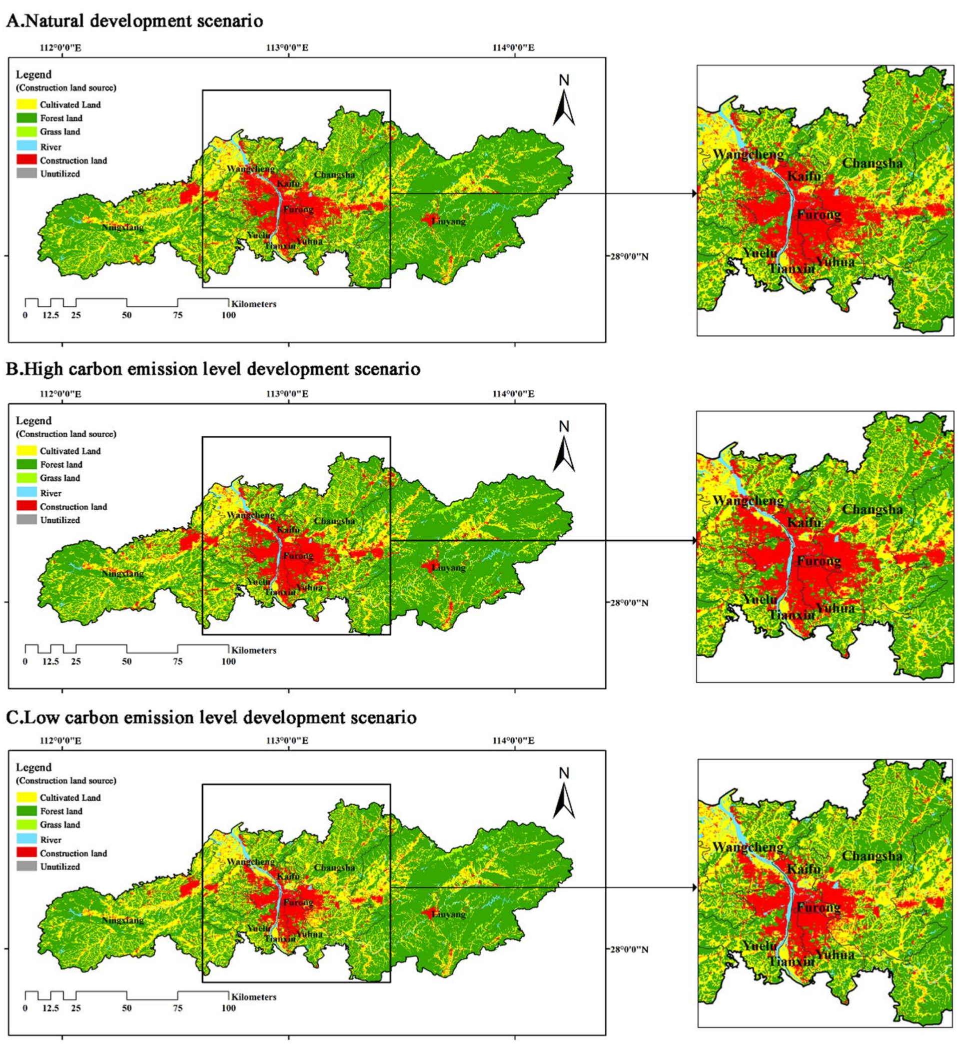

Fig. 8 Distribution of land use in the study area in 2030 under different scenarios

construction land further expands to 1,372.11 km², representing a 49.46% increase compared to the 2020 baseline. In both cases, expansion primarily occurs adjacent to existing urbanized areas, with current construction zones serving as nuclei for outward, peripheral growth. This process contributes to the degradation of key carbon-sequestering ecosystems, including forests, grasslands, and wetlands. Compared to 2020, the area of these ecological lands is projected to decline by 208.56 km² and 256.97 km² under the Natural and High-Emission scenarios, respectively. In contrast, under the Low-Emission scenario—which emphasizes sustainable development and limits ecological land conversion—urban expansion is significantly constrained. By 2030, construction land is projected to reach only 935.51 km², accounting for 7.92% of the total study area.

Assessing the potential effects of construction land growth and its associated carbon emissions control measures

Evaluation of the environmental impact of carbon emissions associated with construction land use

This study evaluates the potential impacts of construction land expansion on regional development in Changsha City from 1990 to 2030, using the IPCC framework for assessing land use change and regional vulnerability. The results (Table 8) indicate that the overall land use intensity in Changsha corresponds to a medium level of development. From 1990 to 2020, the land use intensity index rose from 324.41 to 334.10, representing a 2.99% increase, primarily driven by intensified human activity and economic growth, which accelerated construction land expansion. Meanwhile, total carbon emissions increased as large areas of carbon-sequestering land—such as forests, grasslands, and wetlands—were converted into high-emission land types, including construction land and cropland. This transformation simultaneously heightened emissions and diminished regional carbon sequestration capacity. The potential impact value (PI) for construction land consistently increased from 0.04 in 1990 to a peak of 0.37 in 2015, indicating that construction land expansion has exacerbated carbon emissions and increased ecosystem vulnerability. These developments pose considerable challenges to regional stability, economic growth, and environmental sustainability. In the multi-scenario simulations, both the Natural and High-Emission scenarios show increasing PI values, whereas the Low-Emission scenario demonstrates comparatively lower impacts. When considered alongside changes in the regional elasticity index (EI), results suggest that the Low-Emission scenario provides greater system stability, as the EI values under the other two scenarios increased by 1.21 and 1.22, respectively. These findings underscore that optimizing construction land use, improving energy efficiency, and conserving key carbon-sequestering ecosystems—such as forests and grasslands—can effectively mitigate ecological vulnerability, curb carbon emissions, and support progress toward regional carbon neutrality.

Construction Land Growth Control under Low Carbon Emission Mode

Analyzing the spatiotemporal patterns of regional carbon emissions and their correlation with construction land expansion provides a comprehensive understanding of how urban growth in Changsha City influences carbon output. Based on this analysis, and considering the carbon cycle balance between future development and ecological preservation, the low-carbon development scenario was adopted as the foundation for delineating priority zones for construction land expansion. The selection of this scenario was further supported by potential impact (PI) values and elasticity indices (EI), under which the simulated construction land expansion area was subjected to spatial control. The 2020 construction land layout served as the baseline, defining a guiding zone for regional development covering 918.04 km². The projected expansion area for 2030, totaling 935.51 km²—including the guiding zone—is designated as the priority area for construction land growth and placed under regulatory control.

In terms of spatial configuration (Fig. 9), zone boundaries were delineated based on minimum ecological protection thresholds and the conservation of cultivated land. The expansion follows a radial pattern outward from the guiding zone, integrating fragmented land parcels into a continuous and compact spatial structure. The optimization of construction land regulation within this zone is designed to be dynamic and adaptive, enabling iterative adjustments in response to periodic assessments and evolving planning requirements.

Discussion

Construction land, as the dominant land-use type accommodating urban populations, industrial activity, and transportation infrastructure, can substantially

Table 8 Potential impacts of building land expansion on regional ecosystems

Year	Land use intensity index	Land use intensity change	Total carbon emissions ($\times 10^4$t)	Change in carbon emissions ($\times 10^4$t)	PI	EI
1990	324.41		168.10		0.04	2.76
1995	324.16	−0.25	248.94	80.85	0.02	7.57
2000	324.99	0.83	285.23	36.29	0.04	3.70
2005	325.83	0.84	609.66	324.43	0.13	1.39
2010	330.05	4.22	1164.70	555.04	0.37	0.83
2015	331.98	1.93	1332.69	167.99	0.36	1.00
2020	334.1	2.12	1564.09	231.41	0.04	2.76
2030(Natural development scenario)	340.89	6.79	2396.21	832.12	0.32	1.33
2030(High carbon emission level development scenario)	342.44	8.34	2582.44	1018.35	0.32	1.32
2030(Low carbon emission level development scenario)	334.58	0.48	1639.38	75.29	0.17	2.54

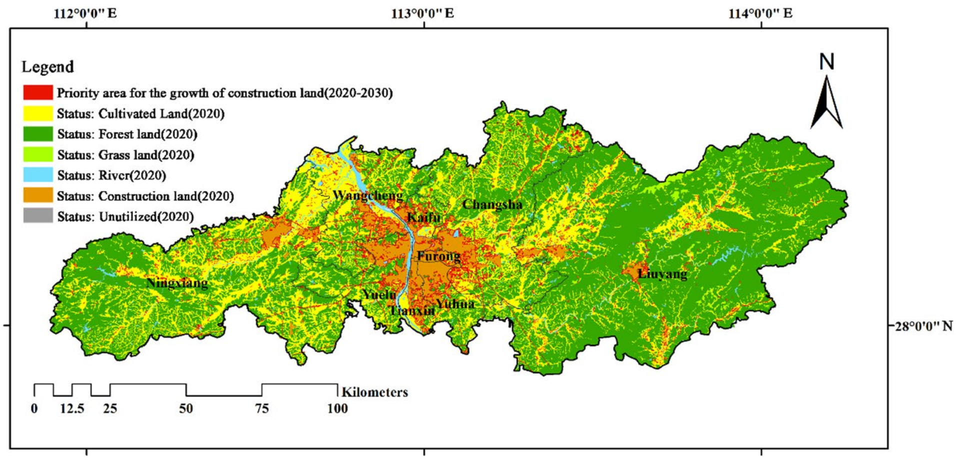

Fig. 9 Priority areas for construction land growth

affect regional carbon emissions, particularly through its expansion. Over the study period, construction-land expansion in Changsha was associated with a net carbon-source effect, consistent with patterns reported for rapidly urbanizing regions [7]. Two complementary mechanisms plausibly explain this pattern. First, construction land typically exhibits substantially higher carbon-emission intensity per unit area than other land-use types; therefore, continued expansion is likely to increase energy use and associated emissions. Second, construction-land expansion often occurs at the expense of high carbon-sink land uses (e.g., forests and grasslands), which can weaken ecosystem carbon-sequestration capacity. Together, higher emissions and reduced sink capacity may amplify pressures on the regional carbon balance. Temporally, from 1990 to 2020, construction land in Changsha expanded by 660.24 km^2. Over the same period, total regional net carbon emissions increased from 1.6810×10^6 t to 1.56409×10^7 t, and the share of emissions attributable to construction land rose from 91.16% to 98.95%. These results indicate that construction land expansion was the dominant contributor to the increase in regional carbon emissions during the study period. The influence of construction-land expansion on carbon emissions peaked around 2010 and moderated thereafter, consistent with Changsha's transition from rapid outward expansion to a phase emphasizing structural optimization; this suggests that the carbon implications of land-development modes vary across urbanization stages. Scenario simulations further indicate that incorporating carbon-emission constraints into construction-land growth regulation can substantially alter the regional emissions trajectory. Moreover, at the scenario simulation level, the differences among the natural development, high carbon development, and low carbon development scenarios are not merely the result of different expansion scales; rather, they represent the combined outcomes of the pathways described above under varying intensities of policy constraints. Under the low-carbon development scenario, both the scale and spatial configuration of expansion are constrained, ecological space is comparatively well protected, and total regional carbon emissions are projected to decline. This outcome is broadly consistent with recent local policies promoting energy-structure adjustment and strengthened ecological-space protection, suggesting that low-carbon-oriented regulation may better align with local development priorities. By contrast, under the high-carbon development scenario, higher emissions per unit construction-land area coincide with substantial losses of high carbon-sink land uses, indicating relatively uncoordinated expansion alongside rapid emissions growth. Therefore, the carbon emission impacts of construction land expansion depend not only on the expansion scale itself but also on its spatial configuration, the level of land use intensification, and the extent to which ecological space is encroached upon. Under continued urbanization, relying solely on controlling expansion scale is often insufficient to stabilize the emissions trajectory. Instead, it is necessary to combine spatial planning control, efficiency improvements, and carbon sink protection to reduce the emission impacts associated with urban expansion. For Changsha, which remains in a phase of ongoing urbanization, an important pathway to mitigate the carbon emission impacts of land expansion is to meet reasonable land demand while optimizing the spatial layout of construction land, increasing land use intensification, and reducing the conversion of ecological carbon sink land.

Methodologically, we propose a coupled Monte Carlo–Markov–PLUS framework to jointly simulate construction-land expansion and carbon-emission responses, integrating uncertainty characterization, land-use quantity projection, spatial allocation, and emissions-response assessment within a single workflow. Within this framework, the transmission pathway from carbon emission scenarios to construction land scale constraints and then to spatial allocation simulation provides a clear interface for embedding policy instruments. At the aggregate level, an emissions cap is translated into a control boundary for the allowable scale of construction land and is introduced as an ex ante constraint in quantity projection, so that construction land growth is subject to a binding carbon target. At the spatial level, bottom line requirements such as the ecological protection redline, permanent basic farmland, and the urban development boundary are operationalized as exclusion or restriction rules. Together with land suitability and neighborhood effects, these rules shape the spatial allocation process by explicitly defining where development is permitted or prohibited. At the intensity level, changes in energy structure and improvements in energy efficiency can be represented in the scenarios through key parameters such as carbon emissions per unit of energy consumption and energy intensity. In implementation, these settings correspond to institutional arrangements including industrial entry requirements, performance evaluation for industrial parks, building energy efficiency standards, and zoning of development intensity, all aimed at reducing emissions per unit of land. In parallel, demand side measures reduce reliance on new construction land by adjusting net demand for additional land and steering optimization within existing built up areas, thereby creating synergy with aggregate, spatial, and intensity constraints. This mapping allows the growth guidance zones and growth priority zones identified under the low carbon scenario to serve not only as simulation outputs but also as planning instruments, which can be translated into differentiated access rules and annual control benchmarks in territorial spatial planning.

Nonetheless, the framework has several limitations. Monte Carlo simulation is sensitive to assumptions about parameter distributions and plausible ranges; alternative specifications—particularly for transition-probability distributions—may affect scenario outcomes. Although repeated random sampling can reduce run-to-run variability, it cannot eliminate uncertainty arising from input-data errors or subjective parameterization. In addition, the spatial accuracy of the PLUS model depends partly on the spatial resolution of land-use data and the selection of driving factors. When resolution is insufficient, the model may fail to capture fine-scale expansion dynamics, potentially leading to underestimation of localized carbon-emission effects. Moreover, non-spatial factors (e.g., policy interventions and market behavior) are represented in a simplified manner, which may limit performance in complex urban-development contexts.

Despite these uncertainties and limitations, this study identifies potential pathways to align construction-land growth regulation with regional carbon-mitigation objectives. The results suggest that steering the direction of construction-land expansion, controlling expansion intensity, and protecting ecological carbon-sink land can reduce emissions pressure associated with urban development. The proposed delineation of priority and guidance zones for construction-land growth offers an operational tool for spatial regulation and supports the integration of carbon-peaking and carbon-neutrality goals into territorial spatial planning. These conclusions are relevant for Changsha in coordinating rational construction-land growth with carbon-peaking targets under ongoing urbanization and may also offer transferable insights for other rapidly urbanizing cities seeking to optimize land-use structure and spatial patterns under carbon-neutrality constraints.

Conclusion and future studies

Conclusion

This study introduces a novel framework that incorporates carbon emissions into the regulation of regional construction land expansion. By examining the spatio-temporal dynamics of construction land transformation and associated carbon emissions in Changsha City from 1990 to 2020, this research explores their interdependent evolution. To project future trends, three scenarios—natural development, high-carbon growth, and low-carbon development—were established to simulate construction land expansion and carbon emissions by 2030. These scenarios assess the potential impacts of construction land growth on carbon emissions and offer targeted strategies for guiding development under a low-carbon trajectory.

(1) From 1990 to 2020, construction land in Changsha expanded cumulatively by 660.24 km^2, following a staged trajectory of "slow initiation–rapid expansion–deceleration." Expansion occurred primarily through the conversion of cultivated land and forest land adjacent to existing construction land; together, these conversions accounted for 95.82% of the newly expanded area. Over the study period, construction-land expansion broadly tracked changes in carbon emissions. Regional net carbon emissions increased from 168.10×10^4 t in 1990 to 1564.09×10^4 t in 2020 (approximately 9.3 times the 1990 level), and the share attributable to construction land rose from 91.16% to 98.95%, indicating that construction land was the dominant source of regional emissions.

(2) Under the three scenarios–business as usual (BAU), high-carbon development, and low-carbon development—projected carbon emissions in Changsha in 2030 are 2396.21×10^4 t, 2582.44×10^4 t, and 1639.38×10^4 t, respectively, representing increases of 53.21%, 65.11%, and 4.81% relative to 2020. Construction-land expansion is pronounced under the BAU and high-carbon scenarios, with increases of 367.85 km^2 and 454.07 km^2,

respectively. By contrast, expansion is strongly constrained under the low-carbon scenario, increasing by only 17.47 km^2 and exhibiting substantially reduced encroachment on high carbon-sink land uses (e.g., forests and grasslands); consequently, both ecological pressure and emissions-growth pressure are comparatively lower.

(3) During 1990–2020, construction-land expansion was consistently associated with higher regional net carbon emissions and was also linked, to some extent, to reduced ecosystem stability. However, after peaking during 2010–2015, this association weakened by 2020, and ecosystem stability showed signs of improvement. Scenario simulations further suggest that in 2030, under the BAU and high-carbon scenarios, ecosystem pressure associated with construction-land expansion is projected to intensify, suggesting a heightened risk of declining ecosystem stability; by contrast, ecosystem stability is projected to improve under the low-carbon scenario. Combined with the delineated priority and guidance zones for construction-land growth under the low-carbon scenario, the low-carbon pathway appears more conducive to balancing ecological, social, and economic objectives while accommodating rational construction-land growth and improving land-use efficiency.

Collectively, these findings provide evidence to support coordinated construction-land development and carbon-emission control and offer practical references for sustainable land-use planning aligned with national carbon-neutrality targets.

Future studies

This study advances a regional approach to regulating construction-land growth by incorporating a carbon-emissions perspective; however, several limitations remain and point to directions for future research. The analysis focuses on the spatiotemporal dynamics of construction-land expansion and associated carbon emissions in Changsha and identifies a strong positive association between the two. Nevertheless, reliance on a single case study may limit the generalizability of the conclusions. Future research should extend the investigation to regions with diverse geographic, economic, and policy contexts to evaluate robustness and to support localized, context-sensitive land-management strategies.

This study employs three scenarios—business as usual (natural growth), high-carbon development, and low-carbon transition—to simulate carbon emissions and construction-land change under alternative development trajectories. However, the scenarios remain stylized and may not fully capture complexities associated with socio-economic dynamics and policy shifts. Future research should incorporate additional variables—such as demographic trends, industrial restructuring, land-market mechanisms, and technological innovation—to improve the precision and policy relevance of simulation results.

Moreover, although this research focuses on the direct impacts of construction-land expansion on carbon emissions, it does not sufficiently address indirect pathways, such as land-use efficiency and spatial optimization. Future studies should examine internal restructuring within construction land, including strategies to improve land-use efficiency, promote compact urban form, and optimize spatial configuration to enhance low-carbon development potential. In addition, the current growth-control strategy is largely driven by carbon-emission metrics, with limited consideration of other ecological indicators (e.g., biodiversity, water resources, and soil quality). Future work should develop multi-objective optimization models that jointly consider carbon mitigation, ecological integrity, and economic development to promote synergistic outcomes in land governance.

Overall, while this study introduces a framework for regulating construction land under carbon-peaking targets, further research is needed to enhance regional applicability, scenario richness, land-use optimization, and multi-objective integration. These efforts will promote deeper integration of territorial spatial planning and low-carbon development and support sustainable urbanization amid a rapidly evolving policy environment.

Author contributions

Z.W.: Writing – review & editing, writing – original draft, validation, methodology, formal analysis, data curation, conceptualization. F.W.: writing – original draft, writing – review & editing, resources, data curation, conceptualization. Z.L.: writing – review & editing, supervision, validation, resources, software, project administration.

Funding

This research was supported by Scientific Research project of Hunan Provincial Education Department (Grant No.23B0246, Grant No.23A0200), The Hunan Provincial Social Science Foundation of China (Grant No. 23YBA113), The Key Discipline of the State Forestry Administration of China (Grant No.21[2016]), The "Double First-class" Cultivation Discipline in Hunan Province(Grant No.469[2018]), The National Long-term Scientific Research Base of Landscape Architecture in Qingxiu Mountain, Nanning, Guangxi, China (Grant No.96[2021]).

Data availability

All relevant data supporting the findings of this study are available on request.

Declarations

Ethics approval and consent to participate

Not applicable.

Consent for publication

Not applicable.

Competing interests

The authors declare no competing interests.

Received: 18 September 2025 / Accepted: 20 March 2026
Published online: 02 May 2026

References

1. Baldassini P, Bagnato CE, Paruelo JM. How may deforestation rates and political instruments affect land use patterns and carbon emissions in the semi-arid Chaco, Argentina? Land Use Policy. 2020;99:104985. https://doi.org/10.1016/j.landusepol.2020.104985.
2. Cai Y, Li K. Spatiotemporal dynamic evolution and influencing factors of land use carbon emissions: evidence from Jiangsu Province, China. Frontiers in Environmental Science. 2024. https://doi.org/10.3389/fenvs.2024.1368205.
3. Chen L, Wang JH, He T, Zhou ZH, Li QR, Yang WW. Forecast study of regional transportation carbon emissions based on SVR. J Transp Syst Eng Inf Technol. 2018;18:13–9. https://doi.org/10.16097/j.cnki.1009-6744.2018.02.003.
4. Deng X, Huang J, Rozelle S, Zhang J, Li Z. Impact of urbanization on cultivated land changes in China. Land Use Policy. 2015;45:1–7. https://doi.org/10.1016/j.landusepol.2015.01.007.
5. Friedlingstein P, Jones M, O'Sullivan M, Andrew R, Bakker D, Hauck J, Le Quéré C, Peters G, Peters W, Pongratz J, Sitch S, Canadell J, Ciais P, Jackson R, Alin S, Anthoni P, Bates N, Becker M, Bellouin N, Zeng J. (2021). *Global Carbon Budget 2021*. https://doi.org/10.5194/essd-2021-386
6. Gomes E, Inácio M, Bogdzevič K, Kalinauskas M, Karnauskaitė D, Pereira P. Future land-use changes and its impacts on terrestrial ecosystem services: a review. Sci Total Environ. 2021;781:146716. https://doi.org/10.1016/j.scitotenv.2021.146716.
7. Gong D, Huang M, Ge Y, Lin H, Zhang L, Altan O. Operationalizing SDGs through the Water-Energy-Food Nexus: multi-level assessment of ecosystem service supply-demand patterns in China. Ecol Ind. 2025;179:114235. https://doi.org/10.1016/j.ecolind.2025.114235.
8. Guo X, Yang J, Shen Y, Zhang X. (2023). Prediction of agricultural carbon emissions in China based on a GA-ELM model [Original Research]. *Frontiers in Energy Research*, *Volume 11–2023*. https://doi.org/10.3389/fenrg.2023.1245820
9. He Y, Piao S, Ciais P, Xu H, Gasser T. Future land carbon removals in China consistent with national inventory. Nat Commun. 2024;15(1):10426. https://doi.org/10.1038/s41467-024-54846-2.
10. Lei F, Yan Y, Yue Y, Bi W, Ni P. The pathway of regional carbon peak in building sector: a case study of Central China. J Build Eng. 2023;80:108031. https://doi.org/10.1016/j.jobe.2023.108031.
11. Li J, Jiao L, Li F, Lu X, Hou J, Li R, et al. Spatial disequilibrium and influencing factors of carbon emission intensity of construction land in China. J Clean Prod. 2023;396:136464. https://doi.org/10.1016/j.jclepro.2023.136464.
12. Liang X, Guan Q, Clarke KC, Liu S, Wang B, Yao Y. Understanding the drivers of sustainable land expansion using a patch-generating land use simulation (PLUS) model: a case study in Wuhan, China. Comput Environ Urban Syst. 2021;85:101569. https://doi.org/10.1016/j.compenvurbsys.2020.101569.
13. Liu J, Peng K, Zuo C, Li Q. Spatiotemporal variation of land-use carbon emissions and its implications for low carbon and ecological civilization strategies: evidence from Xiamen-Zhangzhou-Quanzhou metropolitan circle, China. Sustain Cities Soc. 2022;86:104083. https://doi.org/10.1016/j.scs.2022.104083.
14. Liu Y, Xia C, Ou X, Lv Y, Ai X, Pan R, et al. Quantitative structure and spatial pattern optimization of urban green space from the perspective of carbon balance: a case study in Beijing, China. Ecol Indic. 2023;148:110034. https://doi.org/10.1016/j.ecolind.2023.110034.
15. McCarthy JJ, Canziani OF, Leary N, Dokken DJ, White KS. Climate change 2001: impacts, adaptation, and vulnerability. Contribution of Working Group II to the Third Assessment Report of the Intergovernmental Panel on Climate Change (IPCC). Glob Ecol Biogeogr. 2001;12:87–8.
16. Metzger MJ, Rounsevell MDA, Acosta-Michlik L, Leemans R, Schröter D. The vulnerability of ecosystem services to land use change. Agric Ecosyst Environ. 2006;114(1):69–85. https://doi.org/10.1016/j.agee.2005.11.025.
17. Nesha K, Herold M, De Sy V, Duchelle A, Martius C, Branthomme A, et al. An assessment of data sources, data quality and changes in national forest monitoring capacities in the Global Forest Resources Assessment 2005–2020. Environmental Research Letters. 2021. https://doi.org/10.1088/1748-9326/abd81b.
18. Newbold T, Hudson LN, Hill SLL, Contu S, Lysenko I, Senior RA, et al. Global effects of land use on local terrestrial biodiversity. Nature. 2015;520(7545):45–50. https://doi.org/10.1038/nature14324.
19. Parmesan C, Yohe G. A globally coherent fingerprint of climate change impacts across natural systems. Nature. 2003;421(6918):37–42. https://doi.org/10.1038/nature01286.
20. Pontius RG, Shusas E, McEachern M. Detecting important categorical land changes while accounting for persistence. Agric Ecosyst Environ. 2004;101(2):251–68. https://doi.org/10.1016/j.agee.2003.09.008.
21. Qiu Z, Feng Z, Song Y, Li M, Zhang P. Carbon sequestration potential of forest vegetation in China from 2003 to 2050: Predicting forest vegetation growth based on climate and the environment. J Clean Prod. 2020;252:119715. https://doi.org/10.1016/j.jclepro.2019.119715.
22. Samie A, Abbas A, Azeem MM, Hamid S, Iqbal MA, Hasan SS, Deng X. Examining the impacts of future land use/land cover changes on climate in Punjab province, Pakistan: implications for environmental sustainability and economic growth. Environ Sci Pollut Res. 2020;27(20):25415–33. https://doi.org/10.1007/s11356-020-08984-x.
23. Schröter D, Cramer W, Leemans R, Prentice IC, Araújo MB, Arnell NW, et al. Ecosystem Service Supply and Vulnerability to Global Change in Europe. Science. 2005;310(5752):1333–7. https://doi.org/10.1126/science.1115233.
24. Sun W, Wang C, Zhang C. Factor analysis and forecasting of CO2 emissions in Hebei, using extreme learning machine based on particle swarm optimization. J Clean Prod. 2017;162:1095–101. https://doi.org/10.1016/j.jclepro.2017.06.016.
25. Tian C, Qi L. Empirical decomposition and peaking path of carbon emissions in resource-based areas. J Clean Prod. 2023;395:136372. https://doi.org/10.1016/j.jclepro.2023.136372.
26. Wang S, Liu X, Zhou C, Hu J, Ou J. Examining the impacts of socioeconomic factors, urban form, and transportation networks on CO2 emissions in China's megacities. Appl Energy. 2017;185:189–200. https://doi.org/10.1016/j.apenergy.2016.10.052.
27. Wang Y, Li S, Gu X, Sun Q, Zhang R, Chen F. Spatio-temporal evolution and multi-subject influencing factors of urban green development efficiency in China: Under the carbon neutral vision constraint. Ecol Indic. 2024;167:112580. https://doi.org/10.1016/j.ecolind.2024.112580.
28. Ward A, Yin K-s, Dargusch P, Fulton EA, Aziz AA. The Impact of Land Use Change on Carbon Stored in Mountain Grasslands and Shrublands. Ecol Econ. 2017;135:114–24. https://doi.org/10.1016/j.ecolecon.2016.12.023.
29. Wu H, Yang Y, Li W. Spatial optimization of land use and carbon storage prediction in urban agglomerations under climate change: different scenarios and multiscale perspectives of CMIP6. Sustain Cities Soc. 2024;116:105920. https://doi.org/10.1016/j.scs.2024.105920.
30. Wu Y, Shen J, Zhang X, Skitmore M, Lu W. The impact of urbanization on carbon emissions in developing countries: a Chinese study based on the U-Kaya method. J Clean Prod. 2016;135:589–603. https://doi.org/10.1016/j.jclepro.2016.06.121.
31. Xu S-C, He Z-X, Long R-Y. Factors that influence carbon emissions due to energy consumption in China: decomposition analysis using LMDI. Appl Energy. 2014;127:182–93. https://doi.org/10.1016/j.apenergy.2014.03.093.
32. Xu Z. Towards carbon neutrality in China: a systematic identification of China's sustainable land-use pathways across multiple scales. Sustain Prod Consum. 2024;44:167–78. https://doi.org/10.1016/j.spc.2023.12.008.
33. Yang Y, Liu Y, Li Y, Du G. Quantifying spatio-temporal patterns of urban expansion in Beijing during 1985–2013 with rural-urban development transformation. Land Use Policy. 2018;74:220–30. https://doi.org/10.1016/j.landusepol.2017.07.004.
34. Ye C, Ming T. Land use carbon emissions estimation and carbon emissions control strategy effect scenario simulation in Zhejiang province. Heliyon. 2023;9(11):e20783. https://doi.org/10.1016/j.heliyon.2023.e20783.
35. Zhang D, Wang Z, Li S, Zhang H. Impact of Land Urbanization on Carbon Emissions in Urban Agglomerations of the Middle Reaches of the Yangtze River. Int J Environ Res Public Health. 2021. https://doi.org/10.3390/ijerph18041403.
36. Zhang D, Zhu Z, Chen S, Zhang C, Lu X, Zhang X, et al. Spatially resolved land and grid model of carbon neutrality in China. Proc Natl Acad Sci U S A. 2024;121(10):e2306517121. https://doi.org/10.1073/pnas.2306517121.
37. Zhang S, Zhao T. Identifying major influencing factors of CO2 emissions in China: regional disparities analysis based on STIRPAT model from 1996 to 2015. Atmos Environ. 2019;207:136–47. https://doi.org/10.1016/j.atmosenv.2018.12.040.
38. Zhang X, Zhang D. Urban carbon emission scenario prediction and multi-objective land use optimization strategy under carbon emission constraints. J Clean Prod. 2023;430:139684. https://doi.org/10.1016/j.jclepro.2023.139684.
39. Zhang Y-J, Da Y-B. The decomposition of energy-related carbon emission and its decoupling with economic growth in China. Renew Sustain Energy Rev. 2015;41:1255–66. https://doi.org/10.1016/j.rser.2014.09.021.

40. Zhao P, Zeng L, Li P, Lu H, Hu H, Li C, et al. China's transportation sector carbon dioxide emissions efficiency and its influencing factors based on the EBM DEA model with undesirable outputs and spatial Durbin model. Energy. 2022;238:121934. https://doi.org/10.1016/j.energy.2021.121934.

Publisher's note